PNAS RESEARCH ARTICLE | PHYSICS

Experimental and theoretical evidence of universality in superfluid vortex reconnections

Piotr Z. Stasiak[a,1], Yiming Xing[b,c], Yousef Alihosseini[b,c], Carlo F. Barenghi[a], Andrew Baggaley[a,d], Wei Guo[b,c], Luca Galantucci[a,e], and Giorgio Krstulovic[f]

Affiliations are included on p. 5.

Edited by J.C. Davis, University of Oxford, Oxford, United Kingdom; received December 18, 2024; accepted April 9, 2025

The minimum separation between reconnecting vortices in fluids and superfluids obeys a universal scaling law with respect to time. The prereconnection and the postreconnection prefactors of this scaling law are different, a property related to irreversibility and to energy transfer and dissipation mechanisms. In the present work, we determine the temperature dependence of these prefactors in superfluid helium from experiments and a numeric model which fully accounts for the coupled dynamics of the superfluid vortex lines and the thermal normal fluid component. At all temperatures, we observe a pre- and postreconnection asymmetry similar to that observed in other superfluids and in classical viscous fluids, indicating that vortex reconnections display a universal behavior independent of the small-scale regularizing dynamics. We also numerically show that each vortex reconnection event represents a sudden injection of energy in the normal fluid. Finally we argue that in a turbulent flow, these punctuated energy injections can sustain the normal fluid in a perturbed state, provided that the density of superfluid vortices is large enough.

reconnections | superfluids | vortices | turbulence

Significance

Vortex reconnections are fundamental events that create and sustain turbulence in ordinary fluids (water, air) and in quantum fluids (superfluid helium, Bose–Einstein condensates). In this first joint experimental/theoretical study of reconnections in superfluids, we experimentally demonstrate the time-irreversible character of reconnecting quantum vortices in superfluid helium: their separation dynamics is faster than their approach dynamics. This asymmetry, and its consequent irreversible dynamics, is a universal feature of reconnections, as it has been predicted, numerically, also for other bosonic and fermionic superfluids and for ordinary fluids. Besides the topology, reconnections are also important for the energetics. We find that each reconnection injects superfluid energy into the thermal normal fluid, maintaining it in a dynamically perturbed state.

Reconnections are the fundamental events that change the topology of the field lines in fluids and plasmas during their time evolution. Reconnections thus determine important physical properties, such as mixing and interscale energy transfer in fluids (1), or solar flares and tokamak instabilities in plasmas (2). The nature of reconnections is more clearly studied if the field lines are concentrated in well-separated filamentary structures: vortices in fluids and magnetic flux tubes in plasmas. In superfluid helium this concentration is extreme, providing an ideal context: superfluid vorticity is confined to vortex lines of atomic thickness (approximately $a_0 \approx 10^{-10}$ m); a further simplification is that, unlike what happens in ordinary fluids, the circulation of a superfluid vortex is constrained to the quantized value $\kappa = h/m = 9.97 \times 10^{-8}$ m^2/s, where m is the mass of one helium atom and h is Planck's constant.

It was in this superfluid context that it was theoretically and experimentally recognized (3–9) that reconnections share a universal property irrespective of the initial condition: the minimum distance between reconnecting vortices, $\delta^{\pm}$, scales with time, t, according to the form

$$\delta^{\pm}(t) = A^{\pm}(\kappa|t - t_0|)^{1/2}, \qquad [1]$$

where t_0 is the reconnection time, and the dimensionless prefactors A^- and A^+ refer, respectively, to before ($t < t_0$) and after ($t > t_0$) the reconnection. The same scaling law was then found for reconnections in ordinary viscous fluids (10). In the case of a pure superfluid at temperature $T = 0$ K, theoretical work based on the Gross–Pitaevskii equation (GPE) has shown that $A^+ > A^-$, that is, after the reconnection, vortex lines move away from each other faster than in the initial approach; this result has been related to irreversibility (11, 12). Indeed, a geometrical constraint imposes (12) that a piece of vortex length needs to be "deleted" during the reconnection process. In the GP model, this loss is possible by the emission of a rarefaction pulse created immediately after the reconnection (6, 13) which removes some of the kinetic energy and momentum of the vortex configuration. This vortex energy loss depends on the ratio A^+/A^-, which in turn defines the approaching angle of collision between the vortices, together with other several geometrical quantities (7, 12). The temporal asymmetry $A^+ > A^-$ can be thus interpreted as a nontrivial manifestation of irreversibility, as it originates from an ideal hydrodynamic process independent of the small-scale regularization mechanism of the fluid.

The authors declare no competing interest.

This article is a PNAS Direct Submission.

[1]To whom correspondence may be addressed. Email: p.stasiak@newcastle.ac.uk.

This article contains supporting information online at https://www.pnas.org/lookup/suppl/doi:10.1073/pnas.2426064122/-/DCSupplemental.

Published May 22, 2025.

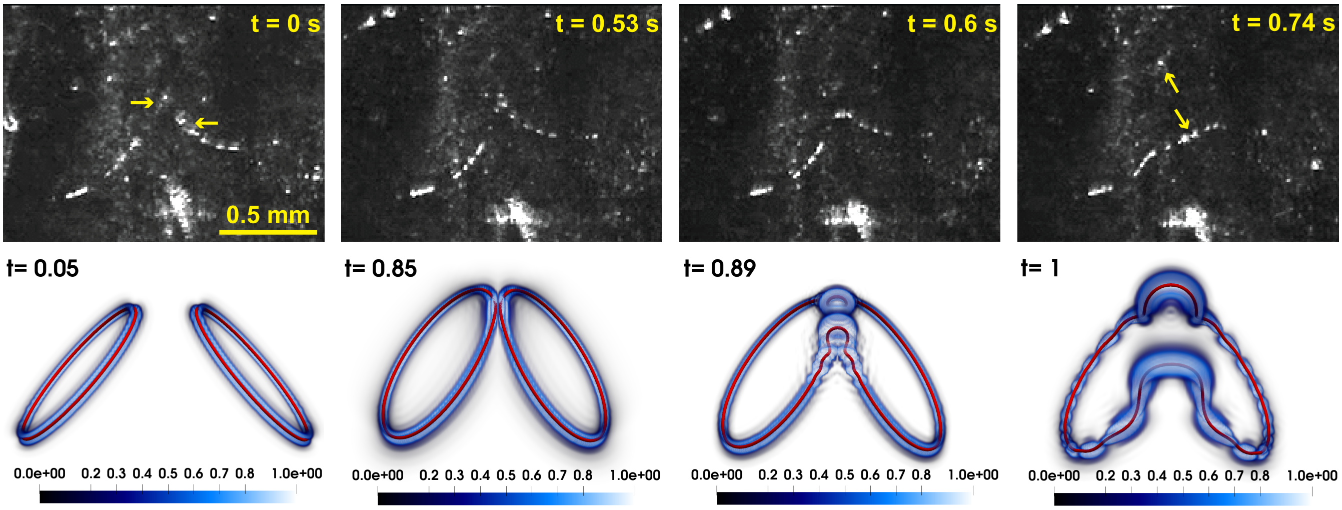

Fig. 1. *Top* row: Images showing tracer particles trapped on reconnecting vortices in superfluid helium at 1.65 K. The arrows denote the vortices before and after the reconnection. The first two images show that the vortices approach each other before the reconnection, which occurs at $t = 0.58$ s. After the reconnection, the resulting vortices start to move apart, as shown in the last two images. *Bottom* row: Oblique collision of two circular vortex rings at different (dimensionless) times, here in units of $\tau = 0.183$s. The superfluid vortex lines are represented by red tubes (the radius has been greatly exaggerated for visual purposes); the scaled normal fluid enstrophy ω^2/ω^2_{max} is represented by the blue volume rendering.

Indeed, in classical fluid vortex reconnections, although the definition of A^+ is more delicate as circulation is not necessarily conserved, the same asymmetry $A^+ > A^-$ was reported (10). Instead of the generation of rarefaction pulses, like in the case of $T = 0$ superfluids, close to the reconnection, the classical fluid creates a series of thin secondary structures that can be then efficiently dissipated by viscous dissipation. We note that the reconnection event also generates wavepackets of Kelvin waves about either side of the reconnection cusp, which propagate outward (visible in the *Bottom* panel of Fig 1). These waves are the fundamental mechanism transferring superfluid kinetic energy to smaller scales (14, 15). The interaction of Kelvin waves with the normal fluid has recently been studied (16, 17).

The case of superfluid helium at nonzero temperatures is more intriguing. Most experiments are performed at $T > 1$ K, a regime in which in addition to quantum vortices, thermal excitations constitute a viscous liquid called the normal fluid. The normal fluid can steal energy from filaments and dissipate it by viscous effects, opening in that way more routes toward irreversibility. Modern visualization techniques rely on hydrogen/deuterium tracer particles to decorate superfluid vortices (4, 18–20). Numerous studies have provided insight into the postreconnection dynamics and the prefactor A^+, but much less is known about A^- from experiments due to the challenges of visualizing vortices approaching a reconnection.

The aim of this Letter is to investigate the role played by the normal fluid in the reconnection dynamics. In particular, given the temperature dependence of the normal fluid's properties, we study experimentally and numerically the temperature dependence of the prefactors A^+ and A^- and numerically investigate the energy injected in the normal fluid. To achieve this aim we need a more powerful model than the GPE to account not only for the dynamics of the superfluid vortices but also for the dynamics of the normal fluid. We show that at nonzero temperatures Eq. **1** and the relation $A^+ > A^-$ hold true, in agreement with experiments, revealing a temperature dependence of A^+/A^-. In addition, we show that a vortex reconnection represents an unusual kind of punctuated energy injection into the normal fluid which acts alongside the well-known (continual) friction. When applied to superfluid turbulence, this last result implies that, if the vortex line density (hence the frequency of reconnections) is large enough, vortex reconnections can maintain the normal fluid in a perturbed state.

Results

Scaling Law. In the experiment, two reconnections were observed where both A^+ and A^- could be identified and calculated, at $T = 1.65$ K and $T = 2$ K, plotted as orange triangles in Fig. 2*B*. We also analyzed six additional experimental observations of the postreconnection dynamics only (vertical dot-dashed lines). All were consistent with the $\delta^{1/2}$ scaling with A^+ in the range 1.2 to 4.2, plotted as vertical lines in Fig. 2*B*. Their corresponding minimal distances are displayed in the *Inset* of Fig 2*A*. The prereconnection factor A^- lies within the 0.4 to 0.6 range, consistent with the results of the numerics, and a clear temperature effect between a superfluid component majority and normal fluid component majority. In the case of the Hopf link, we have performed 147 simulations (49 across 3 temperatures) as shown in Fig. 2*A* and verified Eq. **1** for the minimum distance $\delta^{\pm}$ (21). The prefactors $A^{\pm}$ have been computed in the shaded region of the figure. In the prereconnection regime ($t < t_0$) we observe a clear segregation of the values of A^- due to temperature: the minimum distance grows more rapidly with time if the temperature is lowered. In stark contrast, there is almost no memory of the temperature in the postreconnection regime ($t > t_0$).

At $T = 0$ K, our calculations for superfluid helium (black symbols in Fig. 2*B*) are in good agreement with previous results obtained with the GPE (11) (green diamonds), showing irreversible dynamics. In addition, the computed values of $A^- \approx$ 0.4-0.6 at $T = 0$ K are consistent with analytical calculations (22, 23). At nonzero temperatures, our results confirm the irreversibility of vortex reconnections observed at $T = 0$ as A^+ is always larger than A^-. Importantly, this asymmetry is recovered in all our simulations, regardless of their initial condition. The same asymmetry between A^+ and A^- at nonzero temperatures has been observed for reconnections in finite-temperature

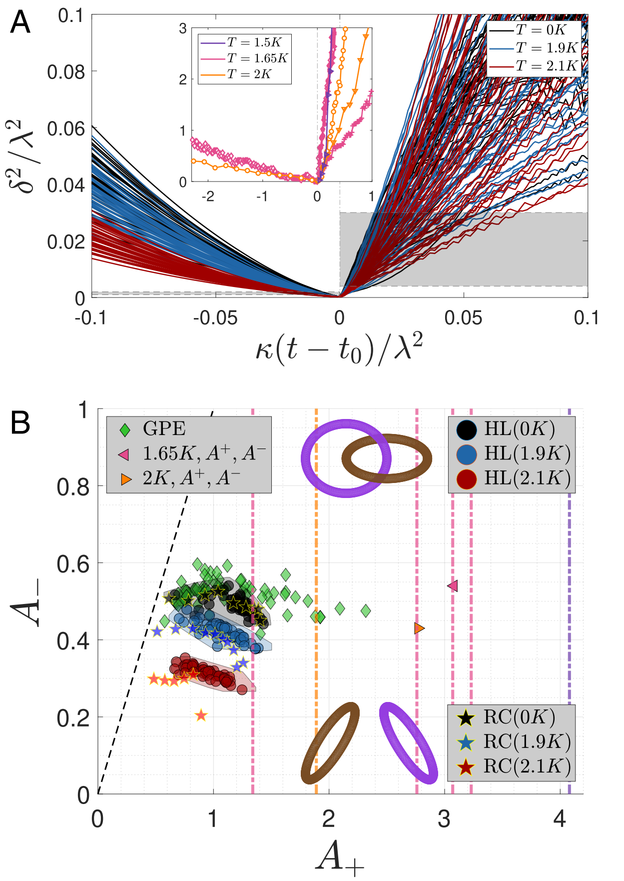

Fig. 2. (*A*) Time evolution of the (dimensionless) minimum distance squared δ^2 plotted vs. (dimensionless) $\kappa(t - t_0)$ for the Hopf link reconnections at $T = 0$ K, 1.9 K, and 2.1 K (black, blue, and red, respectively). The gray shaded areas are the regions used to estimate the prefactors $A^{\pm}$. *Inset*: Experimental superfluid helium data. (*B*) Comparison of all prefactors: Hopf links (*HL*, circles), ring collisions (*RC*, stars with yellow outline), GPE-data from Villois et. al. (11) (green diamonds) and experimental results from this study (triangles and vertical dot-dashed lines). The shaded areas associated with each color represent the convex hull of errors for each temperature and the black dashed line represents the theoretical bound for A^+/A^-. Schematic rendering of initial conditions are included.

Bose–Einstein condensates (24), although in this work the system is not homogeneous (the condensate is confined by a harmonic trap) and the thermal component is a ballistic gas, not a viscous fluid. Note that the vortex reconnections in classical viscous fluids reported in ref. 10 also display a clear $1/2$ power-law scaling for the minimum distance with $A^- \approx 0.3$ to 0.4, which again shows good agreement with our results. The scaling law (Eq. **1**) and the range of values of A^- hence appear to have a universal character in vortex reconnections, independently of the nature of the fluid, classical or quantum.

Energy Injection. The normal fluid impacts the dynamics of reconnecting superfluid vortices via the temperature-dependent mutual friction coefficients. Conversely, the motion of superfluid vortices involved in the reconnection process influences, significantly, the dynamics of the normal fluid. Fig. 3 indeed shows that the normal fluid energy, E_n, suddenly increases at the reconnection time by an amount ($\approx$5%) which is smaller but comparable to the continuous energy increase as vortex lines approach each other. Indeed the curvature $\zeta = |\mathbf{s}''|$ of the vortex line spikes at $t = t_0$ when the reconnection cusp is created, and, in the first approximation (25), the magnitude of the energy injected in the normal fluid per unit time I is proportional to the strength of the mutual friction force $\mathbf{F}_{ns}$ which scales as $|\mathbf{F}_{ns}(\mathbf{s})| \propto |\dot{\mathbf{s}} - \mathbf{v}_n| \propto |\dot{\mathbf{s}}| \propto \zeta$. This sudden transfer of energy (16) from the superfluid vortex configuration to the normal fluid is the origin of the small scale normal fluid enstrophy structures which are visible in Fig. 1.

The total energy injected into the normal fluid by the reconnection, ΔE_n, which hereafter we refer to as the energy jump, is defined as

$$\Delta E_n = \max\left[E_n(t > t_0)\right] - E_n^0, \qquad [2]$$

where $E_n^0 = E_n(t_0)$ is the normal fluid kinetic energy at $t = t_0$. Normalized energy jumps are plotted in Fig. 4 as a function of the ratio A^+/A^-. Here, we observe that the larger A^+/A^- is, the smaller the normal fluid excitation is.

The emission of the sound pulse at the vortex reconnection (13) which is typical of the GPE model is absent in our incompressible hydrodynamic approach. To model this effect, the change of vortex length, ΔL, created by the vortex reconnection algorithm is always negative by construction (26), because, in the local induction approximation to the Biot–Savart law, the superfluid incompressible kinetic energy, E_s, is proportional to the vortex length, L. Such procedure ensures that at $T = 0$ K when a reconnection occurs $\Delta E_s \propto \Delta L < 0$. Consequentially, in the absence of any dissipative normal fluid, the superfluid energy E_s that would be transferred to the sound pulse, normalized with its value E_s^0 at reconnection, is $-\Delta L/L_0$. If these normalized energy jumps (black diamonds in Fig. 4) are compared to the results obtained with the compressible GPE (11) (purple squares) we find a good agreement, confirming that the model we employ, is suitable for the investigation of the features of single reconnection events.

Implications for Turbulence. Our numerical results have implications for our understanding of quantum turbulence (27). A fully developed turbulent tangle of vortices is characterized by its vortex line density $\mathcal{L}$ (vortex length per unit volume); the frequency of vortex reconnections per unit volume is $f = (\kappa/6\pi)\mathcal{L}^{5/2}\ln(\mathcal{L}^{-1/2}/a_0)$ (28). From Fig. 3, we estimate the normal fluid reconnection relaxation time τ_n as the time after reconnection at which the normal fluid energy E_n/E_0

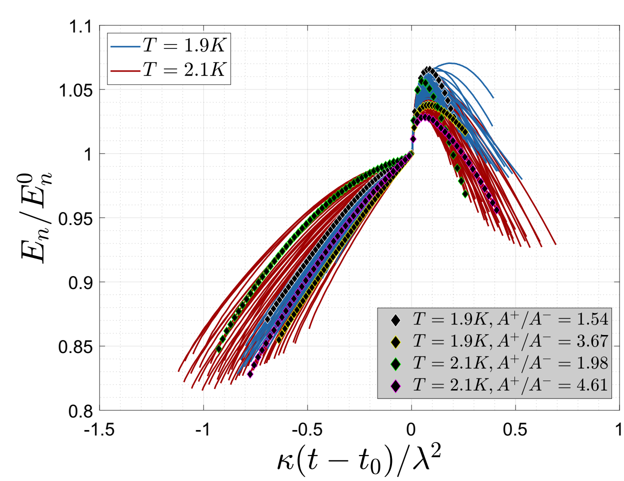

Fig. 3. Normal fluid kinetic energy E_n scaled by E_n^0 (the kinetic energy at $t = t_0$), plotted versus (dimensionless) $\kappa(t - t_0)$ for the Hopf link reconnections. Black diamonds represent the simulations with minimum and maximum prefactor ratios A^+/A^- at $T = 1.9$ K and $T = 2.1$ K, respectively.

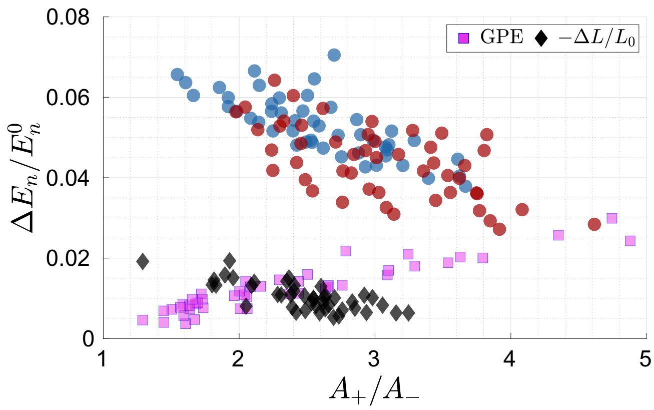

Fig. 4. Normalized energy jumps $\Delta E_n/E_n^0$ for Hopf link reconnections.The solid black diamonds are the normalized change in line length $\Delta L/L_0$ in the $T = 0$ K case. Blue and red circle correspond to $T = 1.9\,K$ and $T = 2.1\,K$ respectively. The purple squares are from GPE simulations of Villois et al. (11).

has decayed to the prereconnection level: in our dimensionless units, $\kappa\tau_n \approx 0.25$. Using this timescale, we estimate that the average vortex line density that is required to sustain the normal fluid in a perturbed state via frequent vortex reconnections is approximately $\mathcal{L} \approx 10^7$ to $10^8\,\mathrm{m}^{-2}$. Experiments in ^{4}He (29–33) and in ^{3}He (34) can achieve vortex line densities much larger than this.

Above the vortex line density threshold, the increase of normal fluid energy generated by the reconnection will not have time to decay before the subsequent reconnection occurs, which will add again more energy. In this manner, the normal fluid energy will not decay to zero, but will increase in time. In general, such finite amplitude normal fluid disturbances constantly injected by reconnections may become relevant for various superfluid helium systems. One example is the oscillatory flows, which are widely studied in superfluid helium using vibrating wires and forks. At low frequency, perturbations which start at finite-amplitude rather than infinitesimal-amplitude level have enough time to become of order one (hence visible and destabilizing) in the supercritical part of the cycle (35). A second example is pipe flow, again relevant to helium experiments, which is known to suffer from finite-amplitude instabilities (36). This effect clearly needs further investigation.

Discussion

We have conducted an experiment using passive particle tracers and a suite of numerical simulations of vortex reconnections over a wide range of temperatures using a model of ^{4}He which accounts for the coupled dynamics of superfluid and normal fluid components. We have verified the scaling law of the minimum vortex distance $\delta^\pm = A^\pm(\kappa|t-t_0|)^{1/2}$ and found that the approach prefactor A^- has a clear temperature dependence independent of the geometry in both experiments and numerics, in contrast to the separation prefactor A^+. The prefactors are in good agreement with GPE simulations (11, 24) and classical fluid reconnections (10) revealing that vortex reconnections display a universal behavior, linked to irreversible vortex energy dissipation, regardless of the nature of the fluid (classical or quantum) and of temperature, i.e., regardless of the small scale energy transfer mechanism. It is worth noting that the behavior, as a function of A^+/A^-, of the energy injected in the normal fluid (at $T > 0$) and of the energy transferred to sound (at $T = 0$) (11, 13) is dissimilar: the former decreases as A^+/A^- increases, the latter the opposite. This likely arises from the distinct physics governing the loss of superfluid incompressible kinetic energy: mutual friction at $T > 0$, quantum pressure at $T = 0$. We have also found that a reconnection event suddenly injects an amount of energy into the normal fluid which is comparable to the energy transferred by friction during the vortex approach. Applying these results to turbulence, we have compared the decay time of the normal fluid structures created by a reconnection to the frequency of reconnections in a vortex tangle, and argued that, if the vortex line density is large enough, these punctuated energy injections should sustain the normal fluid in a perturbed state, which may lead to a new type of turbulence.

Materials and Methods

Experimental Method. To visualize the reconnection dynamics, we decorate the vortices using solidified deuterium (D_2) tracer particles of density $202.8\,\mathrm{kg/m^3}$ (37) and mean radius 1.1×10^{-6} m (38, 39). These particles are generated by injecting a $D_2/^4$He gas mixture into the superfluid helium bath (38, 40) as described in *SI Appendix*. When the particles are near the vortices, they become trapped inside their cores because of the Bernoulli pressure arising from the circulating superfluid flow. A thin laser sheet is used to illuminate the particles, and their motion is recorded at 200 Hz by a camera positioned at a right angle to the laser sheet. A high-quality reconnection event, observed at $T = 1.65$ K and capturing both the pre- and postreconnection dynamics, is shown in Fig. 1 as an example. Note that according to GP simulations (41) the transfer of energy and momentum between particle and vortex does not modify the approaching rates significantly. Reconnection events reported in this work have been captured in multiple experiments, either following particle injection or long time (i.e., 30 to 60 s) after towing a grid through superfluid helium. (this is also supported by the scaling symmetry of the system which allows us to draw conclusion for length-scales relevant to experiments).

Numerical Method. We follow the approach of Schwarz (42) which exploits the vast separation of length scales between the vortex core a_0 and any other relevant distance, in particular the average distance between vortices, ℓ, in the case of turbulence. Vortex lines are described as space curves $\mathbf{s}(\xi, t)$, where ξ is arclength. The equation of motion of the vortex lines is

$$\dot{\mathbf{s}}(\xi, t) = \mathbf{v}_s + \frac{\beta}{(1+\beta)}\left[\mathbf{v}_{ns}\cdot\mathbf{s}'\right]\mathbf{s}' + \beta\mathbf{s}'\times\mathbf{v}_{ns} + \beta'\mathbf{s}'\times\left[\mathbf{s}'\times\mathbf{v}_{ns}\right], \quad [3]$$

where $\dot{\mathbf{s}} = \partial\mathbf{s}/\partial t$, $\mathbf{s}' = \partial\mathbf{s}/\partial\xi$ is the unit tangent vector, $\mathbf{v}_n$ and $\mathbf{v}_s$ are the normal fluid and superfluid velocities at $\mathbf{s}$, $\mathbf{v}_{ns} = \mathbf{v}_n - \mathbf{v}_s$, and β, β' are temperature and Reynolds number dependent mutual friction coefficients (43). The normal fluid velocity $\mathbf{v}_n$ is described as a classical fluid obeying the incompressible ($\nabla \cdot \mathbf{v}_n = 0$) Navier–Stokes equations:

$$\frac{\partial \mathbf{v}_n}{\partial t} + (\mathbf{v}_n \cdot \nabla)\mathbf{v}_n = -\frac{1}{\rho}\nabla p + \nu_n \nabla^2 \mathbf{v}_n + \frac{\mathbf{F}_{ns}}{\rho_n}, \quad [4]$$

where $\mathbf{F}_{ns}$ is the mutual friction force that couples the normal fluid and the superfluid vortices, and acts as an internal injection mechanism. In Eq. **4**, $\rho = \rho_n + \rho_s$, where ρ_n and ρ_s are the normal fluid and superfluid densities, p is the pressure, and ν_n is the kinematic viscosity of the normal fluid. Eqs. **3** and **4** are solved in dimensionless form by rescaling them by the characteristic time τ and length λ. The algorithm for vortex reconnections is standard (26). We consider two distinct initial vortex configurations at three temperatures $T = 0$ K, 1.9 K, and 2.1 K corresponding to the superfluid fractions $\rho_s/\rho = 100\%$, 58%, and 26%. To compare with experiments, the unit of length is set to $\lambda = 1.59 \times 10^{-4}$ m, and the time units to $\tau = 0.183$ s at $T = 0$ K and 1.9 K, and $\tau = 0.242$ s at $T = 2.1$ K; see also *SI Appendix* for details. All configurations lead to a vortex reconnection. The first configuration consists of two vortex rings of (dimensionless) radius $R \approx 1$ in a tent-like shape which collide obliquely making an initial angle α with the vertical direction, as shown in Fig. 1, and, schematically, in Fig. 2*B*. By changing the parameter α, we create a sample of 12 realizations at each temperature (again; see *SI Appendix* for details). The second configuration is the Hopf link, shown schematically in Fig. 2*B*. It consists of two perpendicular linked rings of radius $R \approx 1$ with an offset in the *xy*-plane. By changing the offset, we create a sample of 49 reconnections at each temperature, as described in *SI Appendix*. In all cases, normal fluid structures generated by moving superfluid vortex rings (44), are initially prepared to eliminate any potential transients.

Data, Materials, and Software Availability. Data reported on plots regarding minimum distance and energy injected have been deposited in the Newcastle University Research repository (https://doi.org/10.25405/data.ncl.28727000.v1) (21).

ACKNOWLEDGMENTS. Y.X., Y.A., and W.G. acknowledge the support from the Gordon and Betty Moore Foundation through Grant https://doi.org/10.37807/gbmf11567 and the US Department of Energy under Grant DE-SC0020113. The experimental work was conducted at the National High Magnetic Field Laboratory at Florida State University, which is supported by the NSF Cooperative Agreement No. DMR-2128556 and the state of Florida. G.K. acknowledges financial support from the Agence Nationale de la Recherche through the project QuantumVIW ANR-23-CE30-0024-02. P.Z.S. acknowledges the financial support of French government through the France 2030 investment plan managed by the National Research Agency (ANR), as part of the Initiative of Excellence Université Côte d'Azur under reference number ANR-15-IDEX-01, through the "visiting doctoral student program". Computations were carried out at the Mésocentre Simulations Intensives en Géophysique, Astronomie, Mécanique et Mathématiques hosted at the Observatoire de la Côte d'Azur.

Author affiliations: [a]School of Mathematics, Statistics and Physics, Newcastle University, Newcastle upon Tyne NE1 7RU, United Kingdom; [b]National High Magnetic Field Laboratory, Tallahassee, FL 32310; [c]Mechanical Engineering Department, Florida Agricultural and Mechanical University - Florida State University College of Engineering, Tallahassee, FL 32310; [d]Department of Mathematics and Statistics, Lancaster University, Lancaster LA1 4YF, United Kingdom; [e]Istituto per le Applicazioni del Calcolo "Mauro Picone" - Consiglio Nazionale delle Ricerche, Roma 00185, Italy; and [f]Université Côte d'Azur, Observatoire de la Côte d'Azur, CNRS, Laboratoire Lagrangre, NICE Cedex 4 F-06304, France

Author contributions: P.Z.S., Y.X., Y.A., C.F.B., A.B., W.G., L.G., and G.K. designed research; P.Z.S., Y.X., Y.A., and G.K. performed research; P.Z.S., L.G., and G.K. contributed new reagents/analytic tools; P.Z.S., Y.X., Y.A., W.G., L.G., and G.K. analyzed data; and P.Z.S., Y.X., C.F.B., A.B., L.G., and G.K. wrote the paper.

1. J. Yao, F. Hussain, Vortex reconnection and turbulence cascade. *Annu. Rev. Fluid Mech.* **54**, 317 (2022).
2. I. T. Chapman *et al.*, Magnetic reconnection triggering magnetohydrodynamic instabilities during a sawtooth crash in a tokamak plasma. *Phys. Rev. Lett.* **105**, 255002 (2010).
3. S. Nazarenko, R. West, Analytical solution for nonlinear Schrödinger vortex reconnection. *J. Low Temp. Phys.* **132**, 1 (2003).
4. G. P. Bewley, M. S. Paoletti, K. R. Sreenivasan, D. P. Lathrop, Characterization of reconnecting vortices in superfluid helium. *Proc. Nat. Acad. Sci. U.S.A.* **105**, 13707 (2008).
5. M. S. Paoletti, M. E. Fisher, D. P. Lathrop, Reconnection dynamics for quantized vortices. *Physica D* **239**, 1367–1377 (2010).
6. S. Zuccher, M. Caliari, A. W. Baggaley, C. F. Barenghi, Quantum vortex reconnections. *Phys. Fluids* **24**, 125108 (2012).
7. A. Villois, D. Proment, G. Krstulovic, Universal and nonuniversal aspects of vortex reconnections in superfluids. *Phys. Rev. Fluids* **2**, 044701 (2017).
8. L. Galantucci, A. W. Baggaley, N. G. Parker, C. F. Barenghi, Crossover from interaction to driven regimes in quantum vortex reconnections. *Proc. Nat. Acad. Sci. U.S.A.* **116**, 12204 (2019).
9. M. Tylutki, G. Wlazłowski, Universal aspects of vortex reconnections across the BCS-BEC crossover. *Phys. Rev. A* **103**, L051302 (2021).
10. J. Yao, F. Hussain, Separation scaling for viscous vortex reconnection. *J. Fluid Mech.* **900**, R4 (2020).
11. A. Villois, D. Proment, G. Krstulovic, Irreversible dynamics of vortex reconnections in quantum fluids. *Phys. Rev. Lett.* **125**, 164501 (2020).
12. D. Proment, G. Krstulovic, Matching theory to characterize sound emission during vortex reconnection in quantum fluids. *Phys. Rev. Fluids* **5**, 104701 (2020).
13. M. Leadbeater, T. Winiecki, D. C. Samuels, C. F. Barenghi, C. S. Adams, Sound emission due to superfluid vortex reconnections. *Phys. Rev. Lett.* **86**, 1410–1413 (2001).
14. W. Vinen, Decay of superfluid turbulence at a very low temperature: The radiation of sound from a kelvin wave on a quantized vortex. *Phys. Rev. B* **64**, 134520 (2001).
15. W. Vinen, J. Niemela, Quantum turbulence. *J. Low Temp. Phys.* **128**, 167–231 (2002).
16. P. Z. Stasiak, A. W. Baggaley, G. Krstulovic, C. F. Barenghi, L. Galantucci, Cross-component energy transfer in superfluid helium-4. *J. Low Temp. Phys.* **215**, 324–335 (2024).
17. P. Z. Stasiak *et al.*, Inverse energy transfer in three-dimensional quantum vortex flows. arXiv [Preprint] (2025). https://arxiv.org/abs/2503.04450 (Accessed 6 March 2025).
18. M. S. Paoletti, M. E. Fisher, K. R. Sreenivasan, D. P. Lathrop, Velocity statistics distinguish quantum turbulence from classical turbulence. *Phys. Rev. Lett.* **101**, 154501 (2008).
19. W. Guo, M. La Mantia, D. P. Lathrop, S. W. Van Sciver, Visualization of two-fluid flows of superfluid helium-4. *Proc. Natl. Acad. Sci. U.S.A.* **111**, 4653–4658 (2014).
20. C. Peretti, J. Vessaire, M. Émeric Durozoy, Gibert,, Direct visualization of the quantum vortex lattice structure, oscillations, and destabilization in rotating ^{4}He. *Sci. Adv.* **9**, eadh2899 (2023).
21. P. Z. Stasiak *et al.*, Minimum distance scaling and normal fluid injection during superfluid vortex reconnections in helium-4. Newcastle University Research Repository. https://doi.org/10.25405/data.ncl.28727000.v1. Deposited 6 April 2025.
22. L. Boué, D. Khomenko, V. L'vov, I. Procaccia, Analytic solution of the approach of quantum vortices towards reconnection. *Phys. Rev. Lett.* **111**, 145302 (2013).
23. S. Rica, Self-similar vortex reconnection. *C. R. Méc.* **347**, 365 (2019).
24. A. J. Allen *et al.*, Vortex reconnections in atomic condensates at finite temperature. *Phys. Rev. A* **90**, 013601 (2014).
25. L. Galantucci, G. Krstulovic, C. Barenghi, Friction-enhanced lifetime of bundled quantum vortices. *Phys. Rev. Fluids* **8**, 014702 (2023).
26. A. W. Baggaley, The sensitivity of the vortex filament method to different reconnection models. *J. Low Temp. Phys.* **168**, 18 (2012).
27. C. F. Barenghi, L. Skrbek, K. R. Sreenivasan, *Quantum Turbulence* (Cambridge University Press, 2023).
28. C. F. Barenghi, D. C. Samuels, Scaling laws of vortex reconnections. *J. Low Temp. Phys.* **136**, 281 (2004).
29. K. W. Schwarz, C. W. Smith, Pulsed-ion study of ultrasonically generated turbulence in superfluid ^{4}He. *Phys. Lett. A* **82**, 251–254 (1981).
30. F. P. Milliken, K. W. Schwarz, C. W. Smith, Free decay of superfluid turbulence. *Phys. Rev. Lett.* **48**, 1204–1207 (1982).
31. P. E. Roche, C. F. Barenghi, Vortex spectrum in superfluid turbulence: Interpretation of a recent experiment. *Eur. Phys. Lett.* **81**, 36002 (2008).
32. P. E. Roche *et al.*, Vortex density spectrum of quantum turbulence. *Eur. Phys. Lett.* **77**, 66002 (2007).
33. S. Babuin, E. Varga, L. Skrbek, E. Lévêque, P. E. Roche, Effective viscosity in quantum turbulence: A steady state approach. *Europhys. Lett.* **106**, 24006 (2014).
34. D. I. Bradley *et al.*, Decay of pure quantum turbulence in superfluid ^{3}He-B. *Phys. Rev. Lett.* **96**, 035301 (2006).
35. C. Barenghi, C. Jones, Modulated Taylor–Couette flow. *J. Fluid Mech.* **208**, 127–160 (1989).
36. J. Peixinho, T. Mullin, Finite-amplitude thresholds for transition in pipe flow. *J. Fluid Mech.* **582**, 169–178 (2007).
37. T. Xu, S. W. Van Sciver, Density effect of solidified hydrogen isotope particles on particle image velocimetry measurements of He II flow. *AIP Conf. Proc.* **985**, 191–198 (2008).
38. Y. Tang *et al.*, Imaging quantized vortex rings in superfluid helium to evaluate quantum dissipation. *Nat. Commun.* **14**, 2941 (2023).
39. Y. Tang, S. Bao, W. Guo, Superdiffusion of quantized vortices uncovering scaling laws in quantum turbulence. *Proc. Natl. Acad. Sci. U.S.A.* **118**, e2021957118 (2021).
40. E. Fonda, K. R. Sreenivasan, D. P. Lathrop, Sub-micron solid air tracers for quantum vortices and liquid helium flows. *Rev. Sci. Instrum.* **87**, 025106 (2016).
41. U. Giuriato, G. Krstulovic, Quantum vortex reconnections mediated by trapped particles. *Phys. Rev. B* **102**, 094508 (2020).
42. K. W. Schwarz, Three-dimensional vortex dynamics in superfluid ^{4}He. *Phys. Rev. B* **38**, 2398 (1988).
43. L. Galantucci, A. W. Baggaley, C. F. Barenghi, G. Krstulovic, A new self-consistent approach of quantum turbulence in superfluid helium. *Eur. Phys. J. Plus* **135**, 547 (2020).
44. D. Kivotides, C. F. Barenghi, D. C. Samuels, Triple vortex ring structure in superfluid helium II. *Science* **290**, 777 (2000).